ADVANCES IN SOLAR INPUTS FOR PRECISION ORBIT DETERMINATION

W. Kent Tobiska
Space Environment Technologies
ktobiska@spacenvironment.net
http://www.spacewx.com

AAS/AIAA Astrodynamics Specialists Conference

Lake Tahoe, CA,   **August 7-11, 2005**

AAS Publications Office, P.O. Box 28130, San Diego, CA 92198

ADVANCES IN SOLAR INPUTS
FOR PRECISION ORBIT DETERMINATION

W. Kent Tobiska[†]

Major improvements in solar irradiance specification are reported. These improvements provide more accurate absolute solar energy values, more precise relative variation in solar energy, higher time resolution, and previously uncharacterized energy that affects upper atmosphere densities. These improvements can be applied to precise orbit determination for anomaly resolution and to real-time as well as short-term operational system planning, especially for collision avoidance. After defining the difference between a solar proxy and a solar index, we report on updated background solar extreme ultraviolet (EUV) irradiances and the $E_{10.7}$ and $XE_{10.7}$ indices produced by SOLAR2000 v2.26. These are calibrated to the TIMED/SEE v8 instrument data. We find that the integrated 1–40 nm bandpass energy ($XE_{10.7}$), rather than the full EUV spectrum represented by $E_{10.7}$, has a slightly better correlation with density perturbations. Next, high-time resolution predictions of solar X-ray flare evolution are now being produced operationally and we demonstrate the current state of flare evolution prediction using the X_{b10} and X_{hf} indices. Flares above background irradiances contribute excess energy to atmospheric heating, lead to density changes, affect satellite drag and attitude control. Finally, molecular oxygen dissociates from absorption of far ultraviolet (FUV) energy in the Schumann-Runge Continuum. EUV indicators such as $F_{10.7}$ or $E_{10.7}$ have not previously parameterized the energy in this process and its transfer into the thermosphere. We describe the formation of a new solar index, E_{src} that quantifies energy in the FUV Schumann-Runge Continuum, which can be used to reduce modeled density uncertainties. All five solar indices are compliant with the new ISO 21348 solar irradiance standard.

[†] President and Chief Scientist of Space Environment Technologies, 1676 Palisades Dr., Pacific Palisades, CA 90272-2111. Email: ktobiska@spacenvironment.net. Web site: http://www.spacewx.com. Phone: 310-573-4185. Fax: 310-454-9665.

INTRODUCTION

Solar soft X-ray (XUV: $0.1 \leq \lambda < 10$ nm), Extreme Ultraviolet (EUV: $10 \leq \lambda < 121$ nm), Lyman-alpha ($121 \leq \lambda < 122$ nm), Far Ultraviolet (FUV: $122 \leq \lambda < 200$ nm), Vacuum Ultraviolet (VUV: $10 \leq \lambda < 200$ nm), and Middle Ultraviolet (MUV: $200 \leq \lambda < 300$ nm) spectral irradiances[1] are particularly important for space system engineering, including precision orbit and attitude determination. The energy at these wavelengths is deposited in the thermosphere, mesosphere, and stratosphere. Previous studies[2,3,4] have reported on solar XUV and VUV irradiances characterized by rockets, satellites, and models.

Operational solar irradiance products[5,6,7] have been described in relation to ground- and space-based activities that are affected by space weather. Operational solar irradiance products are solar irradiances and integrated irradiance indices or proxies that are used by space physics models as solar energy inputs in three time frames: past, present, or future. Examples include the use of the 10.7-cm solar radio flux, either as a measured ($F_{10.7}$) proxy or an integrated EUV irradiance ($E_{10.7}$) index, for thermospheric density models including Jacchia-type (Jacchia 1970, CIRA 1972, MET v2.0) or MSIS-type (MSIS-86, MSIS-90, NRLMSIS-00) empirical models. The space systems engineering community often requires precise and accurate operational solar irradiance products for orbit determination in the recent past, at the current epoch, and for the near-term future. Mission critical activities such as collision avoidance monitoring and maneuvering occur in all three time frames. When mission accuracy and precision requirements are not met, this introduces a motivation to provide improved solar irradiance product accuracy, precision, time resolution, cadence, and forecast capability. That motivation is the basis for the development of the integrated irradiance indices described in this paper.

The difference between the terms "proxy" and "index" have often been confused in the literature and it is useful to begin establishing a common set of definitions. As used in this paper, *a solar proxy is a measured or modeled data type that is a substitute for another data type*. An example is the measured 10.7-cm solar radio flux ($F_{10.7}$) that is a substitute for the integrated solar EUV irradiances, which are directly responsible for heating the thermosphere. $F_{10.7}$ does not physically affect the thermosphere. *A solar index is a measured or modeled data type that is an indicator of, or that expresses a level of, solar activity*. An example is the modeled solar EUV integrated irradiance ($E_{10.7}$) that indicates the level of solar chromospheric and coronal activity in the total integrated EUV energy flux bandpass between 1–105 nm.

In the next section we report on the development of more accurate XUV, EUV, FUV, and VUV solar irradiance specifications during the past 3 years. First, increased absolute accuracy and precision of solar irradiance specification is now possible by using new measurements from the TIMED and SORCE missions' solar instruments. Second, improved solar irradiance modeling techniques by EUVAC[8], SunRISE[9,10], NRLEUV[11], and SOLAR2000[12] aid the development and reporting of historical, real-time, and forecast solar irradiances. Third, the improved definition of solar wavelength regions and newly agreed-upon "rules-of-the-road" for comparing instrument measurements with modeled

data now exists with the development of the International Standards Organization (ISO) solar irradiance standard, ISO 21348. Together, these factors provide a strong foundation for improving solar irradiance products useful for space systems engineering.

UPDATED AND NEW SOLAR INDICES

$E_{10.7}$ and $XE_{10.7}$ from SOLAR2000 v2.26

SOLAR2000. SOLAR2000[12] is a collaborative project for accurately characterizing solar irradiance variability across the spectrum. The overarching scientific goal of the SO-LAR2000 (S2K) project is to understand how the Sun varies spectrally and through time from the X-rays through the infrared wavelengths. A primary engineering goal of the S2K project is to provide accurate, precise, and application-specific operational irradiance products, including forecasts, for space systems users. S2K produces irradiances in the spectral range of 1-1,000,000 nm for historical modeling and operational forecasting throughout the solar system. S2K irradiance products such as $E_{10.7}$ (the integrated 1–105 nm solar XUV-EUV) are used as fundamental energy inputs into planetary atmosphere/ionosphere models, for comparison with other solar models, and for modeling or predicting the photon-induced solar radiation component of the space environment.

SOLAR2000, developed by Space Environment Technologies (SET), is presently going through version 2.26 release. The versioning convention (*x.yz*) is the following: "*x*" denotes spectral range variation where v1.yz indicates variability in the XUV and EUV; v2.yz indicates variability into the far ultraviolet (FUV: $122 \leq \lambda < 200$ nm), the middle ultraviolet (MUV: $200 \leq \lambda < 300$ nm), the near ultraviolet (NUV: $300 \leq \lambda < 400$ nm), up to blue light (420 nm); v3.yz indicates variability into the visible (VIS: $380 \leq \lambda < 760$ nm) and infrared (IR: $760 \leq \lambda < 1,000,000$ nm) regions; and v4.yz incorporates physics-based modeling. The "*y*" denotes data improvement status using a multiplicity of instruments (v2.26 is using improved calibrations of the TIMED/SEE v8 data) and the "*z*" denotes code improvement and bug fixes (v2.26 adds improved Lyman-alpha solar cycle specification, code improvements for universal access, and internal algorithm unit consistency). There are several grades of the model. The S2K Research Grade (RG) model, with 550 registered users across 40 countries, provides daily historical data with an approximate 3-month lag before the current epoch. The S2KRG platform-independent GUI application is freely downloadable from the web site http://www.SpaceWx.com. The S2K Professional Grade (PG) GUI application model provides daily historical, nowcast, and forecast data out to 4.5 months (5 solar rotations) which is updated on an hourly cadence. The S2K Operational Grade (OP) server-based model provides daily historical, hourly nowcast, 72-hour (3-hour interval) high time resolution forecast, and daily forecast data out to 5 solar cycles updated on an hourly cadence from SET and NOAA Space Environment Center (SEC) operational servers.

S2K v2.26 is derived using the TIMED/SEE v8 solar EUV data as its calibration reference and has very good correlations with TIMED/SEE in all wavelengths in the EUV. Compared to v2.25, it also has more accurate 27-day solar rotational variation using the TIMED/SEE baseline. The SEE data, for the v2.26 linear regression, extend to lower lev-

els of solar activity; as such, the solar cycle and 27-day rotation trends are distinguished more easily in the longer time series by the derivation algorithm. Figures 1 and 2 demonstrate the XUV-EUV correlations and the excellent comparison with the TIMED/SEE 30.378 nm (He II) emission.
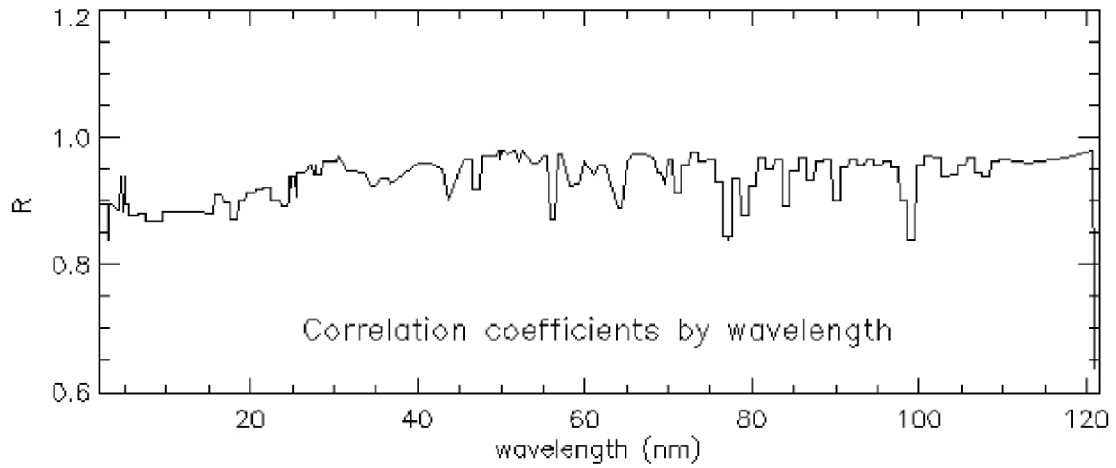

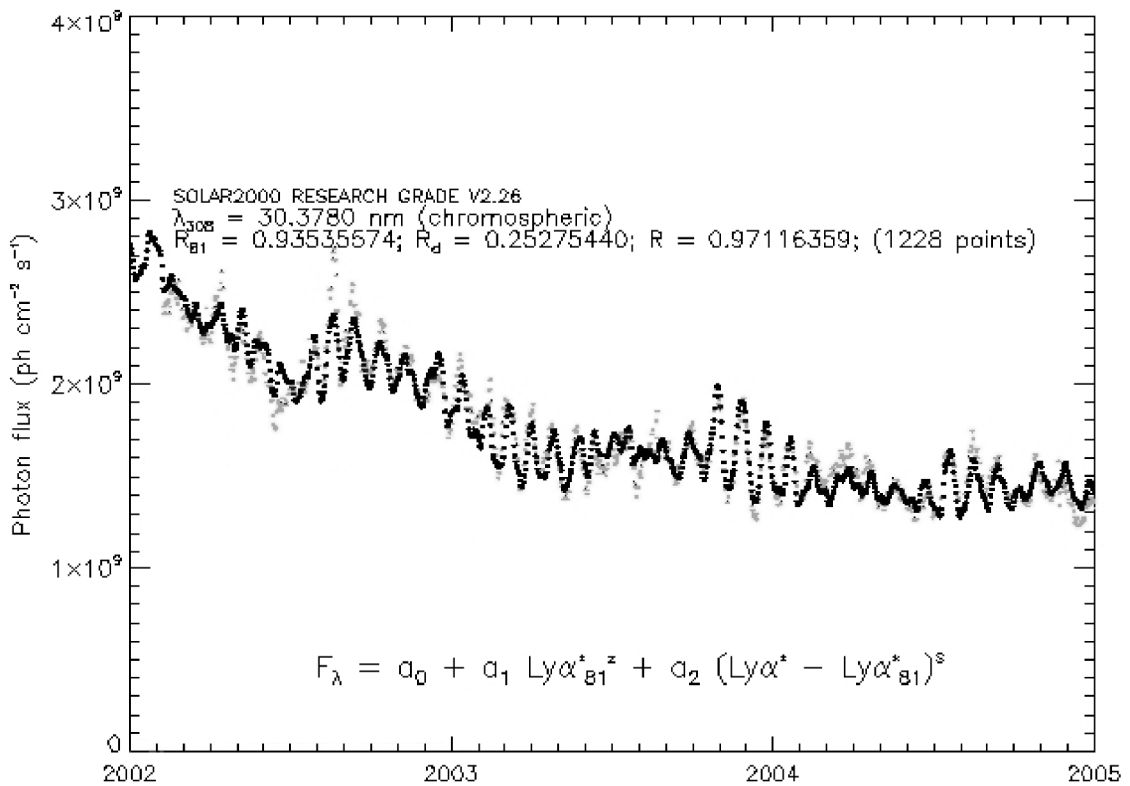Figure 1 Correlations for S2K v2.26 across all XUV–EUV wavelengths.

Figure 2 Comparison between the S2K v2.26 (black dots) and TIMED/SEE (gray) 30.378 nm emission.

4

XE$_{10.7}$. The XE$_{10.7}$ index was first introduced in S2K v2.25 and is updated in v2.26 as described in this paper. It reports the integrated EUV energy flux between 1–40 nm (E$_{1\_40}$) in units of 10.7-cm radio flux[13]. In S2K v2.26, it is derived directly from E$_{1\_40}$ via Eq. (1). XE$_{10.7}$ can be compared to satellite drag data from low inclination (satellite #1616 with a 410 km reference altitude and $i = 36°$) and high inclination (satellite #4122 with a 400 km reference altitude and $i = 77°$) low-Earth orbiting satellites. We have done this for solar maximum to minimum, i.e., January 1, 1990 – December 31, 1996 (F. Marcos, private communication, 2004) and the XE$_{10.7}$ consistently correlates well with drag-derived density. It correlates with density variations the same or slightly better than E$_{10.7}$ and better than F$_{10.7}$. Figures 3 and 4 demonstrate the correlation with density variations using S2K v2.26 E$_{10.7}$, XE$_{10.7}$, and the World Data Center (WDC) F$_{10.7}$ daily observed values where all data for periods of Ap > 7 have been excluded. This isolates the density and solar data comparison to only quiet geomagnetic conditions and allows a focus solely on the solar variability component in comparison with density variations.

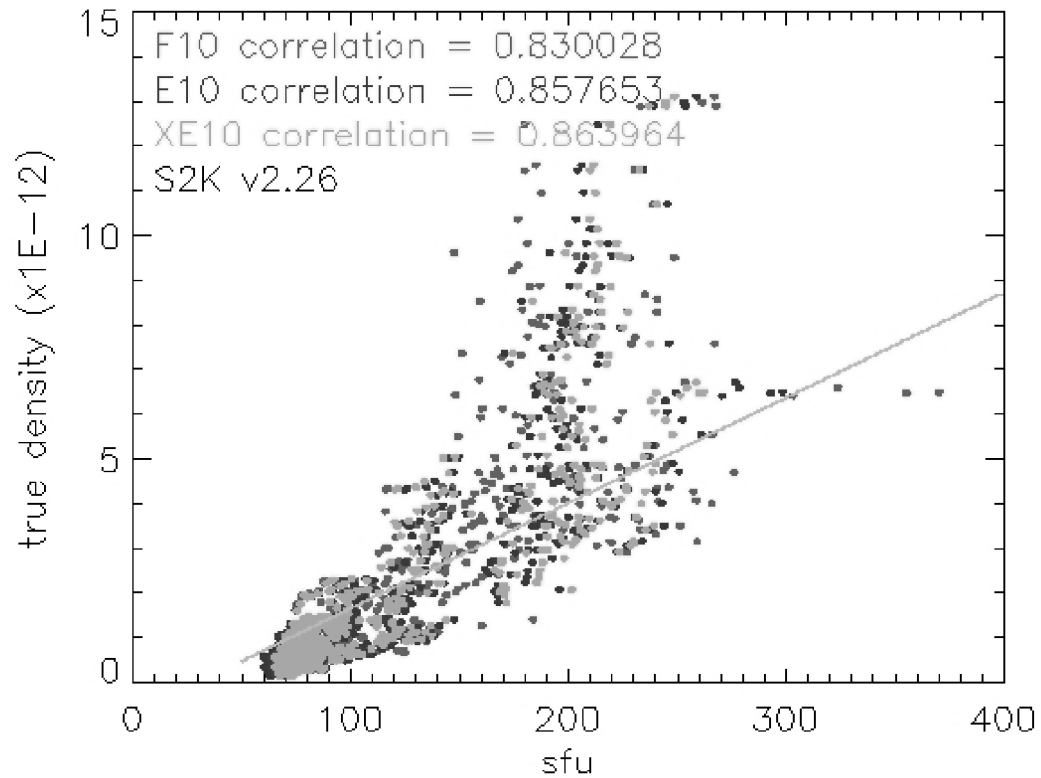$$XE_{10.7} = 16.49 + 43.93 \times E_{1\_40} \quad (\times\ 10^{-22}\ W\ m^{-2}\ Hz^{-1}) \tag{1}$$

Figure 3 Correlations for S2K v2.26 E$_{10.7}$ (0.86), XE$_{10.7}$ (0.86), and F$_{10.7}$ (0.83) with true density from satellite #1616 (i=36°, Ap < 7, 410 km reference altitude).
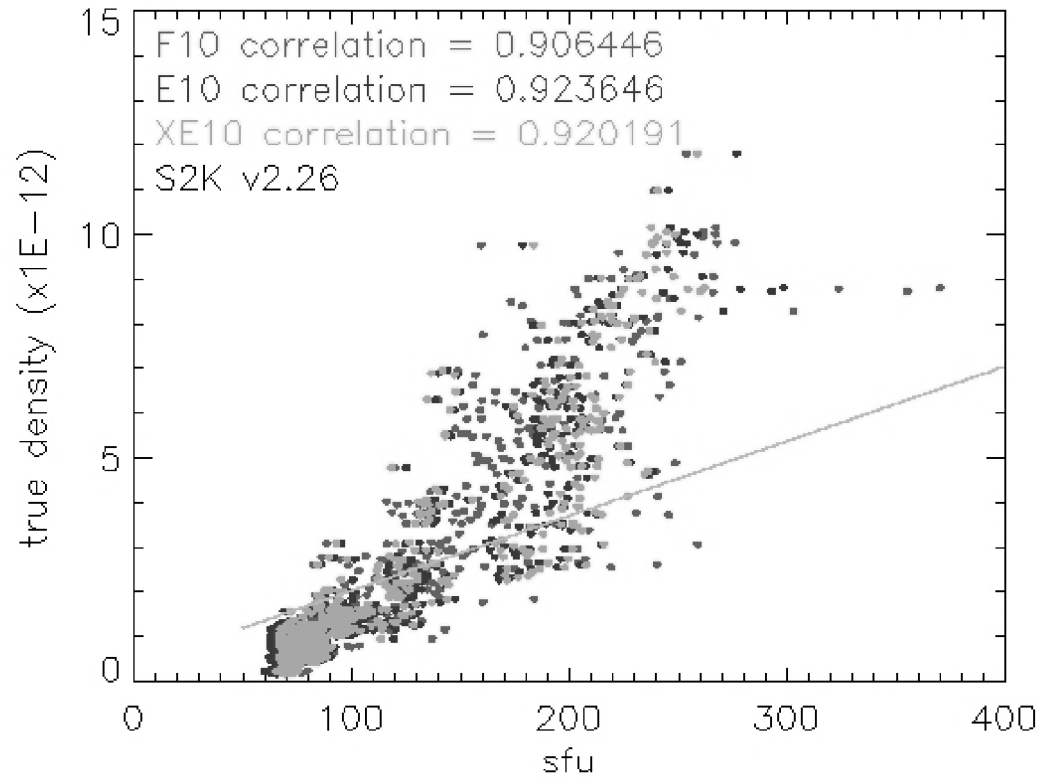
Figure 4 Correlations for S2K v2.26 $E_{10.7}$ (0.92), $XE_{10.7}$ (0.92), and $F_{10.7}$ (0.91) with true density from satellite #4221 (i=77°, Ap < 7, 400 km reference altitude).
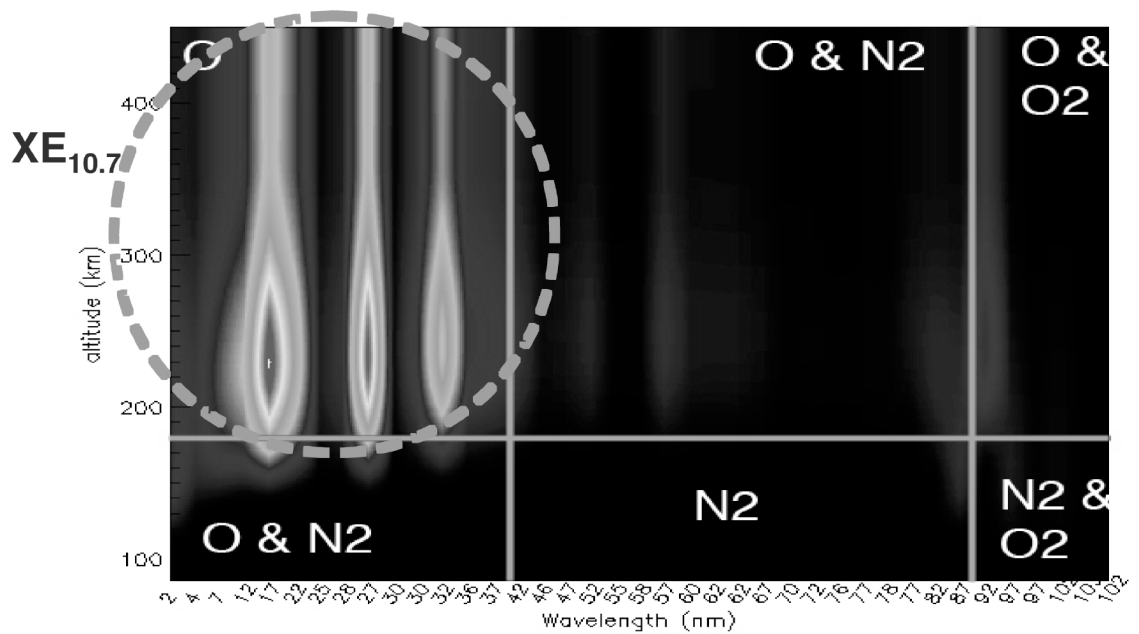

Figure 5 S2K $XE_{10.7}$ quantifies the solar energy from 1–40 nm that preferentially heats atomic oxygen.

The excellent $XE_{10.7}$ correlations for both high- and low-latitude satellites are supported by the fact that between 180–450 km, where these two satellites spend much of their perigee time, the dominant species is atomic oxygen, O, as shown in Figure 5. The 1–40 nm solar energy is the main heating mechanism for the dominant atomic oxygen species at its unit optical depth throughout this altitude region. Therefore, from a physics perspective, using the index ($XE_{10.7}$) that directly expresses the variation in solar energy heating of atomic oxygen, one expects to find a somewhat improved variability compared to $E_{10.7}$ or $F_{10.7}$. $E_{10.7}$ incorporates energy from wavelengths longer than 40 nm that are mostly deposited at altitudes lower than 180 km in an atmospheric region dominated by molecular nitrogen (N_2) and molecular oxygen (O_2).

Xb_{10} and X_{hf} from SOLARFLARE v1.00

Solar spectral irradiances in the bandpass between 0.1–0.8 nm at the short end of the XUV, $XUV_{0.1–0.8}$, consist of a slow time-varying soft X-ray background component (coronal emission above a solar active region) plus a fast time-varying soft X-ray solar flare component. The $XUV_{0.1-0.8}$ is a combination of continuum and lines (free-free bremsstrahlung, free-bound recombination, and two photon emission) dominated by $T>10^6$ K hot corona emission coming from heated plasma in closed magnetic loops within active regions[14,15,16,17]. The energy in this wavelength region is deposited in the 90-100 km lower thermosphere, possibly modulates densities in higher thermosphere layers, and can be highly variable during solar flare events. The irradiance can increase by up to two orders of magnitude in a few minutes from flare start to flare peak and decrease by the same amount over a few hours back to background levels.

These solar energies are measured by the GOES/XRS and are reported by NOAA SEC with a 1-minute cadence and a few-minute lag. Building on the experience of NOAA SEC flare estimates (P. Bornmann, SPD presentation, June 2000), SET utilizes these GOES/XRS data to operationally provide a real-time method for a) identifying the start of solar XUV flares, b) predicting the magnitude and timing of the flare peak, c) predicting the magnitude and timing of the flare decay to half-maximum, and d) predicting the timing of the flare end or duration. The SET model[18], named SOLARFLARE v1.00 as of this paper, operates in real-time and can be accessed via the "Flare Quicklink" at the http://SpaceWx.com web site.

$XUV_{0.1–0.8}$ is a combination of flaring and non-flaring sources. SET first separates the flare and non-flare components to create separate background and flare indices, X_{b10} and X_{hf}.

X_{b10} is the $\log_{10}$ (unitless) number representing the lowest daily decile of the reported GOES $XUV_{0.1–0.8}$ 1-minute data. One-hour of the 1-minute $XUV_{0.1–0.8}$ data is collected and the value of the lowest decile is saved. Over the course of a running 24-hour period, the lowest of the twenty-four decile values is selected as the X_{b10} background value. The resulting X_{b10} index provides the best removal of flare effects we have found. Physically, it represents the $T \approx 10^6$ K coronal emission that gradually evolves on active region time scales. It is likely related to the energy content of the magnetic field frozen in the semi-

stable, slowly evolving active regions and its variability tends to be dominated by the largest of the active regions that are visible on the solar disk. It behaves differently from $F_{10.7}$, which is created in the cooler, $T \approx 10^4$ K transition region.

X_{hf} is the $\log_{10}$ (unitless) number representing the difference between the daily (previous running 24-hours) X_{b10} background value, created hourly, and the median of the $XUV_{0.1-0.8}$ measurements each hour. This index provides a good estimate of $10^6 < T < 10^7$ K hot coronal flare activity. Its short-lived variability tends to be dominated by individual flares or the largest of simultaneous flares. Figure 6 shows X_{b10} and X_{hf} separated from each other for October-November 2003.
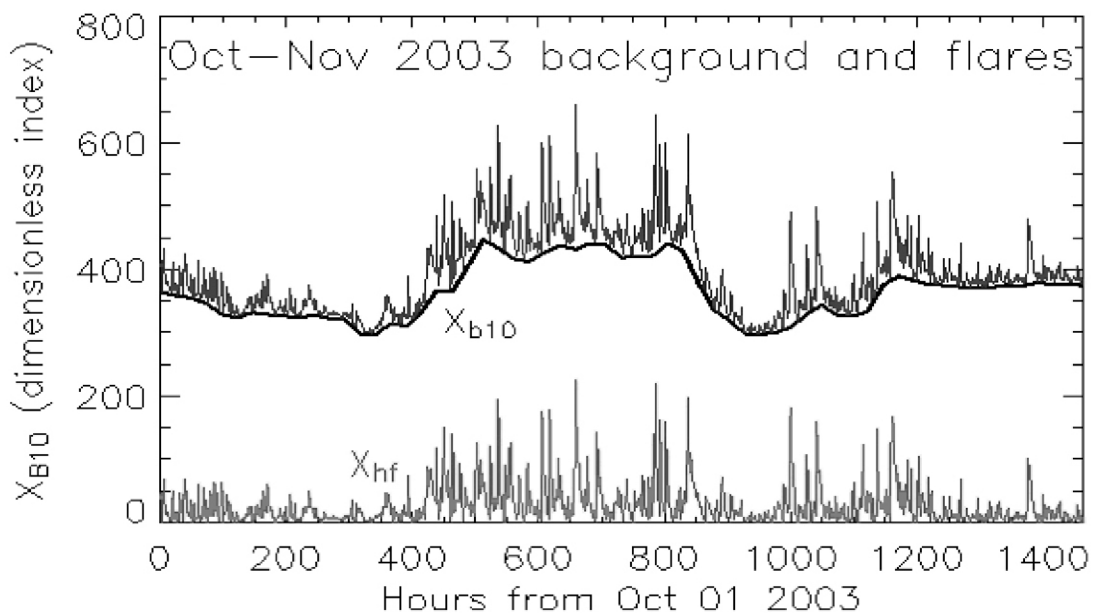

Figure 6 The X_{b10} (mid-range dark line) and X_{hf} (lower gray line) during the October-November 2003 solar storm period. The highly variable upper gray line is the combined X_{b10} and X_{hf} that is temporally identical to the GOES/XRS $XUV_{0.1-0.8}$.

The time rate of change of X_{hf}, dX_{hf}/dt, is calculated every 2-minute operational cycle so that the actual flare start time, rise phase, and decay shape can be determined. Tobiska and Bouwer[18] describe in more detail the development of these indices and Figure 7 shows the SOLARFLARE v1.00 predictive results for July 24-27, 2005.

In summary, the SET SOLARFLARE v1.00 operational model (Flare Quick-link at http://SpaceWx.com) creates the X_{b10} and X_{hf} indices and is able to capture fast-rising XUV flares every 2 minutes. When a flare is detected, the model predicts the flare's 1-minute time evolution over the subsequent 4–6 hours for use by space systems operations (Figure 8). The X_{b10} and X_{hf} indices, having a 2-minute cadence, a 2–9 minute real-time lag, and predictive time resolution of 1-minute for 6 hours into the future, are excellent tools for use in precise orbit determination and collision avoidance strategies during pe-

riod of active solar flares. They are real-time, short-term predictive indices that express the minutes-to-hours effects of solar soft X-ray flares upon the density variations of the lower thermosphere, which can couple with the higher atmosphere layers and ionosphere.
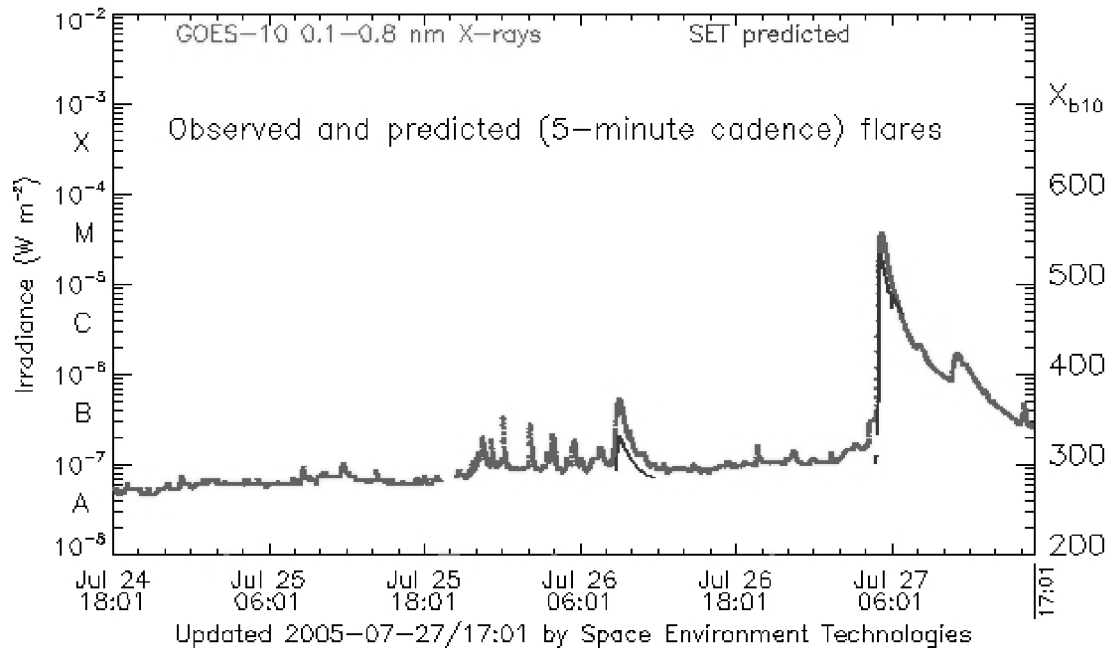

Figure 7 The SOLARFLARE v1.00 flare evolution prediction model results (black lines) compared with 1-minute GOES/XRS XUV 0.1-0.8 data (gray dots) for July 24-27, 2005.
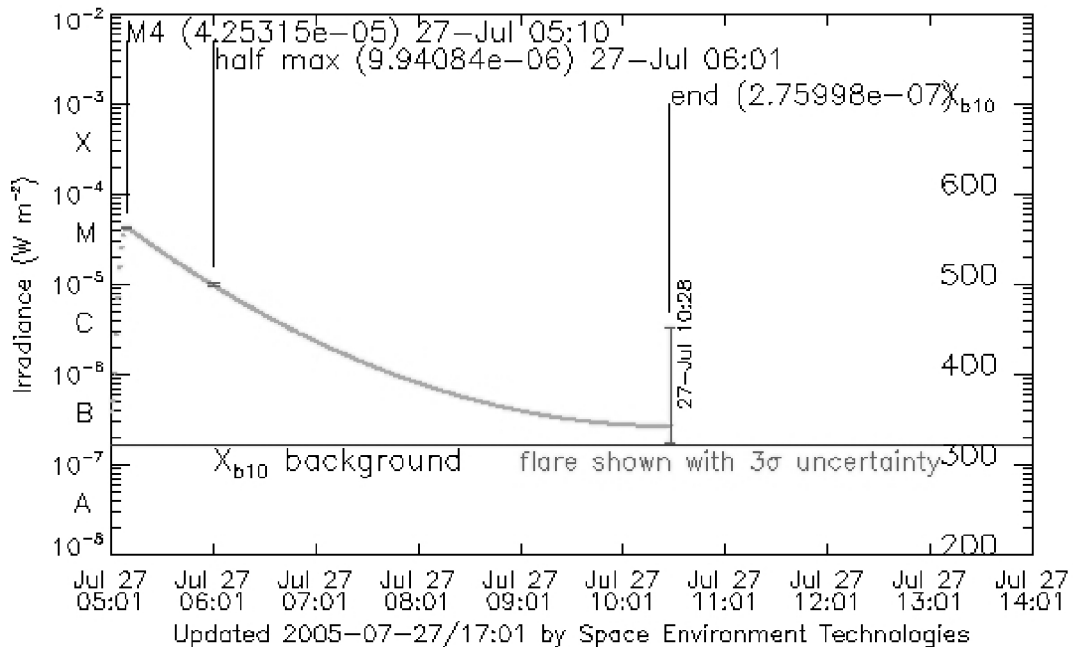

Figure 8 The SOLARFLARE v1.00 flare evolution prediction model for a July 27, 2005 M-class flare.

E$_{src}$ from UARS, TIMED, SORCE

Schumann-Runge Continuum. The Schumann-Runge Continuum (SRC) covers the 125–174 nm solar spectral wavelength range and is a solar FUV continuum emission. Unit optical depth of this solar energy extends through the lower thermosphere (90-120 km) where the SRC is the major cause of molecular oxygen, O_2, dissociation (Figure 9). When O_2 dissociates, the free atomic oxygen can recombine with other species in the lower thermosphere or be transported elsewhere due to the effects of differing recombination rates with various species as well as non-solar forces such as dynamics (gravity waves, planetary waves, winds, tides, and inter/intra-hemispheric circulation) and species transport from coupled ionosphere-magnetosphere processes (Joule heating, charged particle precipitation, plasma drifts).

Because of the complexity of these interactions, the net effect of SRC perturbations affecting the overlaying thermosphere neutral densities has not been well understood. In this paper, we describe a new solar index, the E$_{SRC}$, which parameterizes the energy content of the SRC, is reported in units of 10.7-cm solar flux, and is found to be useful for reducing residuals of neutral density uncertainty after the semi-annual variation and the solar EUV effects have been removed (Bruce Bowman, private communication, 2005). In attempting to understand potential contributions to density variations by the SRC, we have created several test cases of SRC energy. The first task was to create a time series of SRC energy that can be compared with satellite-derived density variations.
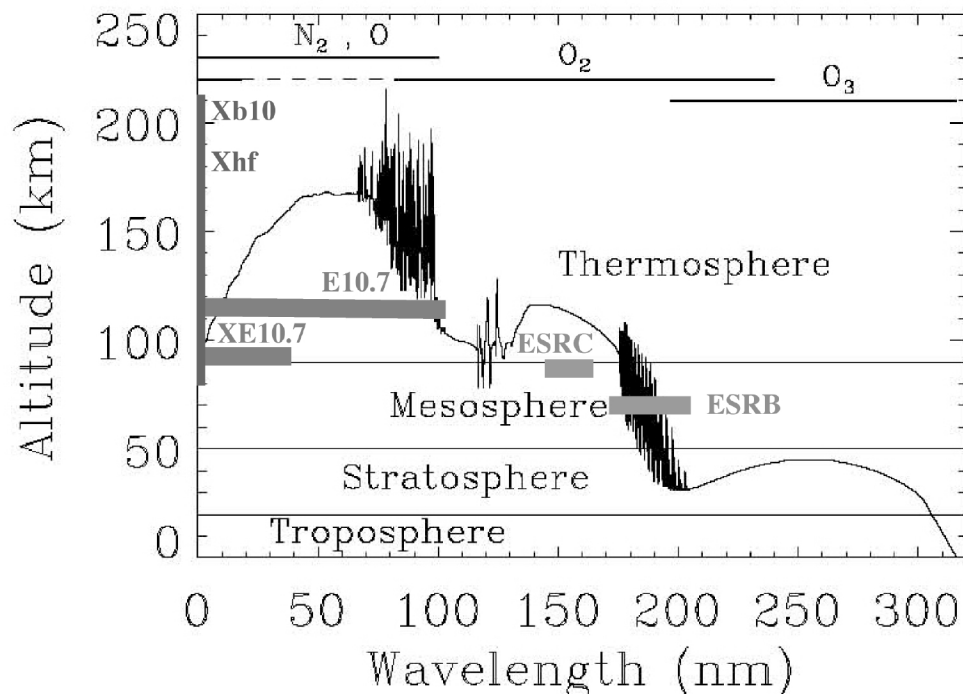

Figure 9 Unit optical depths for the XUV–MUV solar spectrum showing the SRC range covered by the E$_{SRC}$. Other solar indices are also shown. (Figure is annotated from a template provided by T. Woods.)

FUV data and E_{SRC} formation. The UARS/SOLSTICE[19] v18 and v19, TIMED/SEE[20] v8, and SORCE/SOLSTICE[21] v5 missions/instruments provide the FUV time series. The version refers to dataset calibrations. These instruments were built and operated by the Laboratory for Atmospheric and Space Physics (LASP) at the University of Colorado. The datasets are publicly available for scientific and engineering research from LASP or from each mission's archives. Figure 10 shows the data availability from these 3 missions.

After collecting the LASP raw data from the 3 missions, and as a precursor to forming the E_{SRC} index, we compiled a composite dataset for each 1-nm wavelength bin between 125-175 nm. As part of the compilation, it was necessary to readjust and scale the separate 1-nm wavelength bin datasets to remove instrument changes. In consultation with the LASP instrument PI teams, we developed and implemented, in this order, the following steps: a) scaled the TIMED/SEE v8 data to the overlapping SORCE/SOLSTICE v5 data; b) scaled the combined TIMED and SORCE data to the overlapping UARS/SOLSTICE v19 data; c) scaled the combined TIMED, SORCE, and UARS/SOLSTICE v19 data to the overlapping UARS/SOLSTICE v18 data; d) rescaled the combined 4 datasets using 5th degree polynomial fits for each combined dataset ensemble of 1-nm bins and Lyman-alpha that, when convolved, established consistent solar cycle trends; and e) ensured that each 1-nm wavelength bin magnitude of solar cycle variation from solar minimum (1996) to the average of solar maximum (1991 and 2000), using the 5th degree polynomial fits, was retained throughout the rescaling. Figure 11 shows an example of the individual datasets prior to and after readjustment for the 155-156 nm wavelength bin.
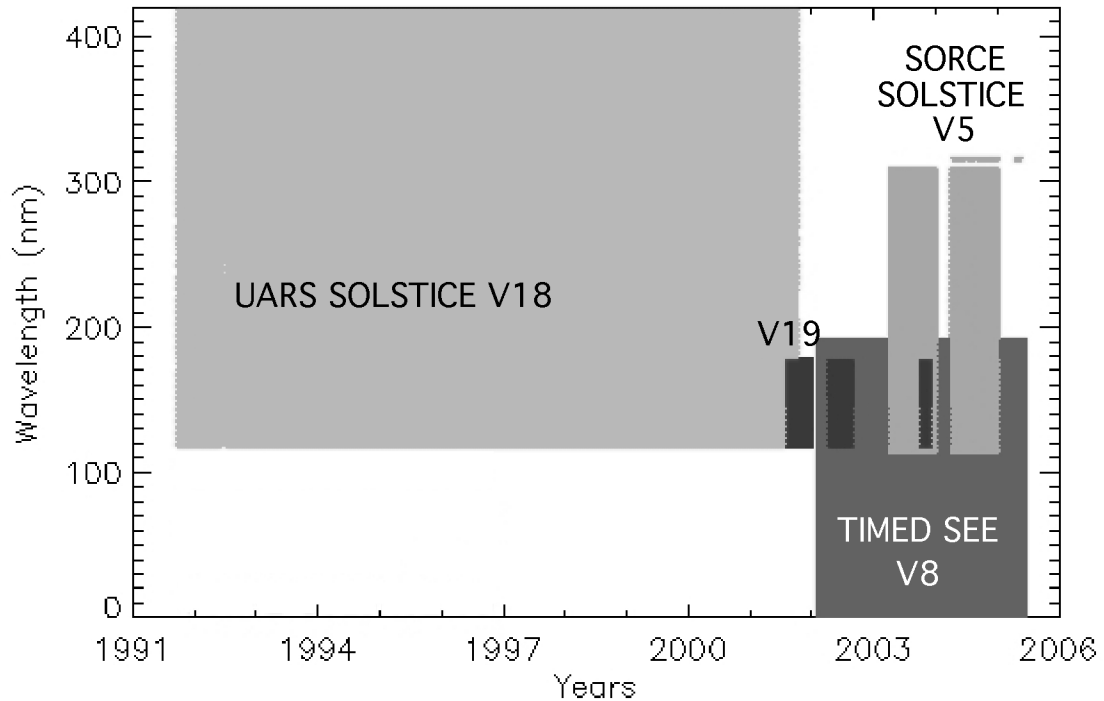

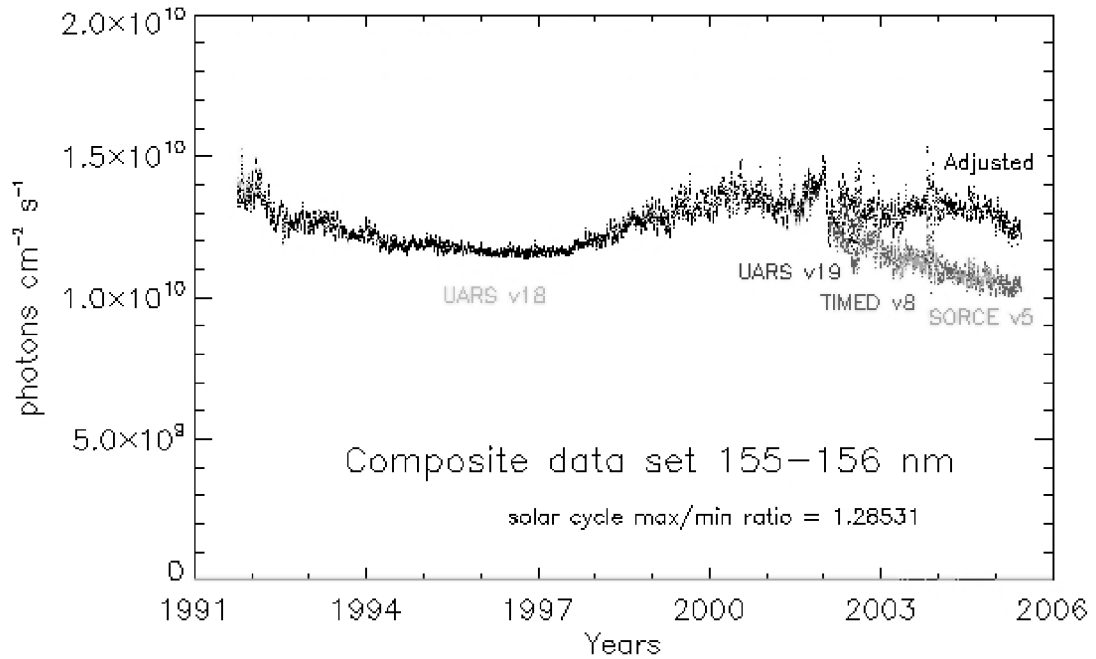Figure 10 Data availability from the UARS, TIMED, and SORCE missions.

Figure 11 Unadjusted and readjusted solar 155-156 nm data from UARS, TIMED, and SORCE datasets.

After the successful formation of 1-nm wavelength bin composite datasets, we formed the E_{SRC} index. Four versions of this index were developed and tested including the fully integrated 125-175 nm wavelength range, the 144-145 nm bin, the 151-152 nm bin, and the integrated 145-165 nm range. In each case, the readjusted, composite photon flux (photons cm^{-2} s^{-1}) in each wavelength bin or bandpass was integrated across the entire bin or bandpass and then fit to the 10.7-cm radio flux using a 1st degree polynomial fit. The resulting index is the integrated SRC in a particular bandpass reported in units of 10.7-cm radio flux ($\times 10^{-22}$ W m^{-2} Hz^{-1}). It was determined (Bruce Bowman, private communication, 2005) that the 145-165 nm and 125-175 nm broadband ranges performed the best in reducing density variation uncertainties. We have adopted the 145-165 nm range as the E_{SRC} index since, for future satellite missions, it may be easier to develop a detector using a 145-165 nm broadband filter rather than a spectrally resolved instrument. Figure 12 presents the resulting 145-165 nm bin E_{SRC} index.

In summary, the new E_{SRC} index is provided to better characterize, especially for operations, the coupling between solar energy deposition in the lower thermosphere and atmospheric density variability. The physical processes of energy transfer are still being studied but, at a minimum, include the photodissociation of lower thermospheric molecular oxygen into free atomic oxygen. The latter may contribute to time-lagged upper thermosphere density enhancement as a result of energy transfer via species photochemical recombination, dynamical transport (vertical, meridional, or zonal winds, waves, tides, interhemispheric circulation), diffusion (eddy, turbulent or molecular), thermal conduction, or coupled ionosphere-magnetosphere processes.
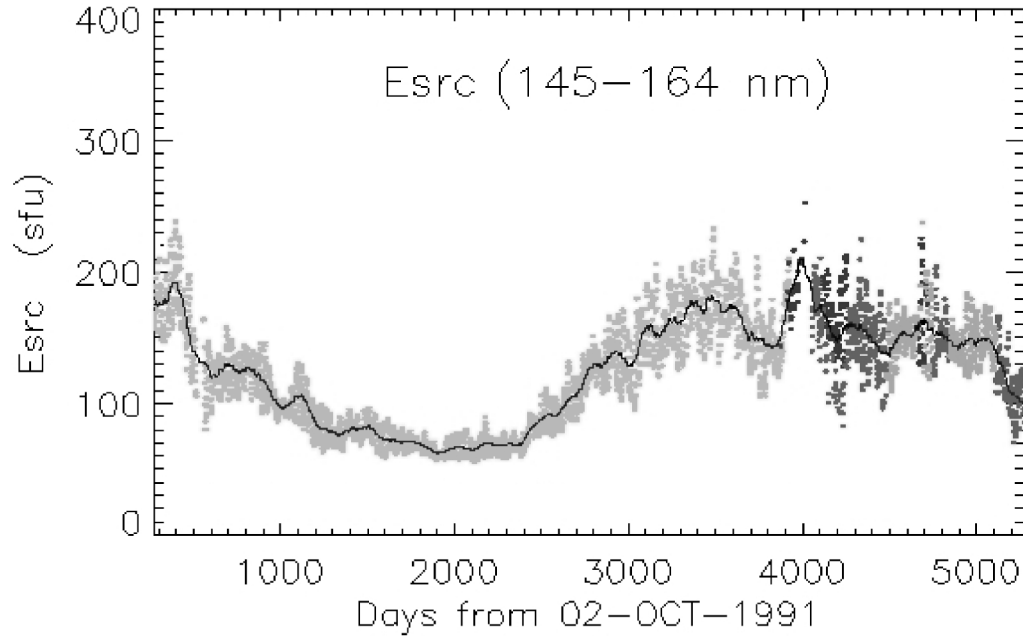
Figure 12 E_{SRC} solar index as a composite time series from the UARS, TIMED, and SORCE datasets. The 81-day smoothed values are shown as a solid line. Shades of gray denote the 4 datasets.

SOLAR INDICES' COMPLIANCE WITH ISO 21348

The International Standards Organization (ISO) International Standard (IS) 21348 "Space environment (natural and artificial) – Process for determining solar irradiances" specifies the process for determining all representations of solar irradiances and irradiance products. This includes the use of models such as SOLAR2000 v2.26 and SOLARFLARE v1.00, as well as satellite-measured FUV irradiances from UARS, TIMED, and SORCE, that provide solar irradiances, indices, and measured data, respectively. Collectively, these are known as solar irradiance products.

The processes described herein for determining solar irradiance products are compliant with ISO 21348. The SOLAR2000 v2.26 integrated irradiance $E_{10.7}$ and $XE_{10.7}$ indices, the SOLARFLARE v1.00 X_{b10} and X_{hf} indices, and the E_{SRC} index derived from the composite UARS, TIMED, and SORCE datasets have an ISO 21348 type 5 designation. They provide solar irradiance temporal variation information for integrated bandpasses. ISO 21348 can be viewed in draft form at the "ISO solar standard" link at http://www.SpaceWx.com. A description of the evolution of and details about this standard is provided by Tobiska and Nusinov[1].

CONCLUSION

We describe five solar indices that represent major improvements in solar irradiance specification. Prior to discussions of the solar indices, we define the terms *solar proxy* and *solar index* where a solar proxy is a measured or modeled data type that is a substi-

tuted for another data type ($F_{10.7}$) and a solar index is a measured or modeled data type that is an indicator of, or that expresses a level of, solar activity ($E_{10.7}$).

The first two indices, $E_{10.7}$ and $XE_{10.7}$, have been improved to provide more accurate absolute solar energy values and more precise relative variation in solar energy. They come from the most current release of SOLAR2000, v2.26, and provide improved 27-day variation compared with previous versions of the indices. In comparisons between satellite-derived density data, $F_{10.7}$, $E_{10.7}$, and $XE_{10.7}$, the latter correlates as well as or better than the other solar proxies/indices with the density data. $XE_{10.7}$ is the integrated energy between 1–40 nm reported in $F_{10.7}$ units that directly heats atomic oxygen, which is the dominant neutral atmospheric species between 180–450 km.

The second two indices, X_{b10} and X_{hf}, are produced from the GOES XRS $XUV_{0.1-0.8}$ 1-minute data by the SOLARFLARE v1.00 model developed by SET. The X_{b10} removes flare effects and physically represents the $T \approx 10^6$ K coronal emission that gradually evolves on active region time scales. X_{hf} is the difference between the daily (previous running 24-hours) X_{b10} background value created hourly and the median of the $XUV_{0.1-0.8}$ measurements each hour. It provides a good estimate of $10^6 < T < 10^7$ K hot coronal flare activity. Both indices have a 2-minute cadence, a 2–9 minute real-time lag, and predictive time resolution of 1-minute for 4–6 hours into the future. They are excellent tools for use in precise orbit determination and collision avoidance strategies during periods of active solar flares.

The fifth index, E_{SRC}, is formed from the readjusted composite UARS/SOLSTICE v18/v19, TIMED/SEE v8, and SORCE/SOLSTICE v5 datasets and is the integrated photon flux between 145–165 nm in the FUV Schumann-Runge Continuum. It is reported in $F_{10.7}$ units and its energy is deposited directly into the lower thermosphere between 90–120 km. It is the primary source of molecular oxygen, O_2, photodissociation and has been created to operationally characterize the coupling between solar irradiance energy deposition in the lower thermosphere and upper thermosphere density variability. The photodissociation of lower thermospheric molecular oxygen into free atomic oxygen may contribute to time-lagged upper thermosphere density enhancement, i.e., a previously uncharacterized energy process affecting upper atmosphere densities in satellite drag calculations.

The improvements described here provide more accurate absolute solar energy values, more precise relative variation in solar energy, higher time resolution, and previously uncharacterized energy that may affect upper atmosphere densities. An immediate application of these improved solar indices is to precise orbit determination for anomaly resolution. Real-time and short-term forecast indices for use by operational systems can aid in collision avoidance for low Earth orbit spacecraft.

ACKNOWLEDGEMENT

lar Standard" link, the SOLAR2000 model is available at the "S2KRG Quick-link", and SOLARFLARE real-time flare evolution predictions are available at the "Flare Quick-link" on the http://www.SpaceWx.com web site.

REFERENCES

1. Tobiska, W.K. and A.A. Nusinov, Status of ISO draft international standard for determining solar irradiances (DIS 21348), *J. Adv. Space Research*, in press, 2005.
2. Woods, T., L. Acton, S. Bailey, F. Eparvier, H. Garcia, D. Judge, J. Lean, D. McMullin, G. Schmidtke, S. Solomon, K. Tobiska, and R. Viereck, Solar extreme ultraviolet and X-ray irradiance variations, *AGU Monograph,* 10.1029/141GM11, 127-140, 2004.
3. Tobiska, W.K., SOLAR2000 irradiances for climate change research, aeronomy, and space system engineering, *Adv. Space Research*, **34** (8), 1736-1746, 2004.
4. Woods and Rottman, Solar ultraviolet variability over time periods of aeronomical interest, in *Comparative Aeronomy in the Solar System,* eds. M. Mendillo, A. Nagy, and J. Hunter Waite, Jr., Geophys. Monograph Series, Wash. DC, pp. 221-234, 2002.
5. Tobiska, W.K., E10.7 use for global atmospheric density forecasting in 2001, AIAA 2002-4892, *AIAA Aerospace Sciences Meeting*, Reno, NV, January, 2002.
6. Tobiska, W.K., Forecast E10.7 for Improved LEO Satellite Operations, *J. Spacecraft Rock.,* **40** (3), 405-410, 2003.
7. Tobiska, W.K., Forecasting of space environment parameters for satellite and ground system operations, AIAA 2003-1224, *AIAA Aerospace Sciences Meeting*, Reno, NV, January, 2003.
8. Richards, P.G., J.A. Fennelly, and D.G. Torr, EUVAC: A solar EUV flux model for aeronomic calculations, *J. Geophys. Res.*, **99**, 8981-8992, 1994.
9. Fontenla, J.M., O.R. White, P.A. Fox, E.H. Avrett, and R.L. Kurucz, Calculation of solar irradiances. I. Synthesis of the solar spectrum, *Astrophys. J.,* **518,** 480-499, 1999.
10. Fox, P.A., J.M. Fontenla, O.R. White, and K.L. Harvey, Calculation of solar irradiances II. Synthesis, *Astrophys. J.,* in press, 2004.
11. Warren, H.P., J.T. Mariska, and J. Lean, A new model of solar EUV irradiance variability. 1. Model Formulation, *J. Geophys. Res.,* **106,** 15745-15758, 2001.
12. Tobiska, W.K., T. Woods, F. Eparvier, R. Viereck, L. Floyd, D. Bouwer, G. Rottman, and O.R. White, The SOLAR2000 empirical solar irradiance model and forecast tool, *J. Atm. Solar Terr. Phys.,* **62,** 14, 1233-1250, 2000.
13. Tobiska, W.K. and S.D. Bouwer, New developments in SOLAR2000 for space research and operations, *J. Adv. Space Research*, in press, 2005.
14. Mewe, R., *Solar Phys.,* **22**, 459, 1972.
15. Kato, T., *Astrophys. J. Suppl. Ser.,* **30**, 397, 1976.
16. Mewe, R. and E.H.B.M. Gronenschild, Calculated X-radiation from optically thin plasmas. IV - Atomic data and rate coefficients for spectra in the range 1-270 Å, *Astron. Astrophys. Suppl, Ser.,* *45*, 11, 1981.
17. Aschwanden, M., Irradiance observations of the 1–8 Å solar soft X-ray flux from GOES, *Solar Phys.,* **152**, 53-59, 1994.
18. Tobiska, W.K. and S.D. Bouwer, Solar flare evolution model for operational users, *IES 2005 Proceedings,* ed. J.M. Goodman, in press, 2005.
19. Woods, T. N., G. J. Ucker, and G. J. Rottman, SOLar STellar Irradiance Comparison Experiment: 2. instrument calibration, *J. Geophys. Res., 98*, 10679, 1993.
20. Woods, T.N., S. Bailey, F. Eparvier, G. Lawrence, J. Lean, B. McClintok, R. Roble, G.J. Rottman, S.C. Solomon, and W.K. Tobiska, TIMED Solar EUV Experiment, *Phys. Chem. Earth,* **25,** No. 5-6, 393-396, 2000.
21. Woods, T., G. Rottman, J. Harder, G. Lawrence, B. McClintock, G. Kopp, and C. Pankratz, Overview of the EOS SORCE mission, *SPIE Proceedings*, *4135*, 192, 2002.